# Threshold for Radiation Effects in Silica*

William Primak

*Argonne National Laboratory, Argonne, Illinois* 60439

Data are given for the initial compaction (negative dilatation) of vitreous silica per incident bombarding ion for 40- and 140-keV $H^+$, $D^+$, $He^+$, $Ne^+$, $Ar^+$, and 80-keV $He^+$. The slope of the logarithm of these data plotted against the logarithm of the energy above a threshold value dissipated in nuclear scattering indicates that the threshold energy for the compaction process is very low; much below the typical displacement threshold energy $\sim 25$ eV. In contrast, when Hines and Arndt's data for the disordering of quartz in ion bombardment are treated in a similar fashion, a threshold energy $\sim 25$ eV is obtained.

## I. INTRODUCTION

This is one of a group of related investigations of the radiation-induced dilatations of vitreous silica. The immediate antecedants of this one are four published papers.[1-4] In the second is a historical account pertinent to this paper.

Very small dilatations are conveniently measured photoelastically.[5] A specimen thicker than the range is irradiated on one face, and the dilatation can be calculated from the induced anomalous birefringence. The ranges of ions of energies of interest here are $\sim 1$ $\mu$ or less; hence the birefringence induced in a typical specimen, 2–4 mm thick, is very small. The possibility of performing the present investigation arose through an improvement of an order of magnitude in the sensitivity of our instrumentation.[6]

For most solids, dilatations are not easily interpreted. In vitreous silica they result largely from movement of oxygens with a consequent alteration in void space, and a fraction is contributed by associated changes in polarizability of the oxygen ions.[7] Negative dilatations in vitreous silica may be caused by many agents and are referred to as compactions (hence, $-\Delta V/V$, where $V$ is the volume). Such agents may be ionization (hence, ionization compaction), corpuscular radiation (hence, corpuscular compaction), or others.

The mechanism for the radiation compaction of vitreous silica is still controversial. It would be helpful to know the threshold energy for the process. Displacement threshold energies are usually determined through electron bombardment. However, this method cannot be used for vitreous silica because of the ionization compaction.[8] Recently it was found that the ionization and corpuscular compactions progress by different laws, the efficiency of the former falling off greatly as it progresses.[2] Thus it seemed possible that a threshold energy could be obtained from the ion-bombardment data. The principles had been utilized long ago in inverse in a graphite study.[9] As the present data

were being accumulated, papers prepared from Lindhard and Scharff's[10,11] treatment of the ranges of low-energy ions became available, and this greatly simplified the analysis.

## II. EXPERIMENTAL

The material studied was the vitreous silica Suprasil. It was cut to blocks about $1.2 \times 1.2 \times 0.3$ cm, and lapped and polished on all faces.

Ion bombardments were performed in a Cockcroft–Walton machine in the manner described in previous papers.[2] It had been fitted with a new larger analyzing magnet, thus permitting the work with $Ne^+$ and $Ar^+$ reported here. Although fairly consistent results were obtained in a particular run, data obtained at different times showed some fluctuation, indicating systematic errors. A voltage ripple in the accelerator power supply which caused the beam to oscillate across the target Faraday cup has been discovered, and recently another worker using the machine found evidence of neutral atoms in the beam. Steps to remedy these problems have been taken and should improve the quality of future data. The precision required for the present application is very low because the data will be utilized on a logarithmic scale. Some caution should be exercised, however, in making other applications of this data.

The principles of measuring the dilatation are reviewed in a recent paper.[5] The instrumentation employed in the present investigation is also described in detail,[6] and typical recorder tracings of birefringence across the thicknesses of bombarded specimens are shown. The birefringence varies linearly across the thickness $W$ of the bombarded specimen. The experimental quantity required is $z$, the difference in birefringence at the two edges. The edges were not sufficiently well defined in the recorder tracings. The quantity $z$ (degrees rotation of the analyzer in the de Senarmont compensator arrangement) was therefore obtained by measuring the slope of the curve and then multiplying it by the measured value of the specimen thickness

TABLE I. Radiation compaction of vitreous silica.

| Ion | Energy (keV) | Compaction ($V_{oxy}$/ion) | | Dissipation (keV) | | | Lindhard range $\mu$ |
|-----|-----|-----|-----|-----|-----|-----|-----|
| | | Raw | Corrected[a] | Energy ionization | Total nuclear | Nuclear >30 eV | |
| H+ | 140 | 30 | 26 | 138.9 | 1.135 | 0.602 | 1.174 |
| | 40 | 15 | 16 | 39.0 | 0.976 | 0.504 | 0.604 |
| D+ | 140[b] | 67 | 59 | 137.2 | 2.74 | 1.768 | 1.594 |
| | 40 | 82 | 92 | 37.6 | 2.29 | 1.468 | 0.790 |
| He+ | 140[b] | 210, 246[c] | 210, 244[c] | 132.0 | 8.54 | 6.86 | 1.06 |
| | 40[b] | 210 | 166 | 34.0 | 6.44 | 5.18 | 0.482 |
| Ne+ | 140[b] | 1551 | 1656 | 63.4 | 68.8 | 66.6 | 0.307 |
| | 80[b] | 1431 | 1316 | 27.6 | 48.5 | 46.7 | 0.179 |
| | 40 | 842 | 1038 | 9.70 | 28.9 | 27.6 | 0.091 |
| Ar+ | 140 | 2105 | 2233 | 36.7 | 103.3 | 100.9 | 0.155 |
| | 40 | 1473 | 2046 | 5.60 | 34.4 | 33.4 | 0.046 |

[a]Corrected for saturation (see text).
[b]Select data (see text).

[c]Data for two configurations of the Cockroft–Walton machine.

W. The quantity of interest here is the total effect caused by the incident ions, the integral of the dilatation over the range $t$. It is given by

$$\bar{\delta}t = \tfrac{1}{6}(2.818 \times 10^{-6})\,(W/D)z/(1.7 \times 10^{-23}),$$

where the last factor converts the units of dilatation to oxygen volumes $(V_{oxy})$; $\bar{\delta}$ is the mean dilatation over the range $t$; and the factors on the right-hand side of the equation are first, a geometric one; second, a product of elastic and photoelastic constants appropriate for the light employed, mercury green, 0.546 $\mu$; and $D$ is the length of the specimen in the optical path of the photoelastimeter.

*Note added in proof.* The unit oxygen volumes have proven helpful in interpreting the effect[21] but have no significance in the present paper.

The individual data for these bombardments are too numerous to present here; consisting of several runs for each ion and each energy. The results for the initial stages of compaction, whether exponential or a reduced power-law dependence, are linear when plotted on log-log paper (for typical curves see Ref. 2). A logarithmic least-squares curve was fitted to the points obtained in a progressive bombardment; and the slope in degrees (analyzer rotation) per microcoulomb (taken as $6.25 \times 10^{12}$ charges) was calculated. This was converted to $V_{oxy}/\mu$C with the aid of the above equation. The results are given in Table I.

### III. DISCUSSION

Calculations of the stopping of the incident ions were based on the papers by Lindhard *et al.*,[10,11] to which the reader is referred for descriptions of the formulas presented below. The stopping was calculated separately for the ion moving through silicon and oxygen of the respective densities of these atoms in vitreous silica and were then added. The familiar formulas were used as follows and

incorporated in a machine calculation[12]:

$$\epsilon = 33.09[M_2(M_1+M_2)^{-1}](Z_1Z_2Z^{1/2})^{-1}E,$$

$$\rho = 2.861 \times 10^{-16}N[M_1M_2(M_1+M_2)^{-2}]Z^{-1}R,$$

$$k = 0.0793\,Z_1^{1/6}(Z_1Z_2)^{1/2}Z^{-3/4}[(M_1+M_2)^3M_1^{-3}M_2^{-1}],$$

where $\epsilon$ is in ergs, $E$ in keV, and $\rho$ in cm. The total stopping $S_T$ has two major terms: an electronic term and a nuclear scattering term $s(\epsilon)$;

$$S_T = [s(\epsilon)+k\epsilon^{1/2}](E/\epsilon)(\rho/R).$$

Numerical results for $s(\epsilon)$ and $f(t^{1/2}) \equiv f(\zeta)$ are tabulated.[11] For machine calculation the following approximations were used:

$$s(\epsilon) = 0.3578912 - 0.1781634v - 0.152256v^2$$
$$+ 0.0475905v^3 + 0.04562v^4 + 0.0076472v^5,$$
$$0.002 < \epsilon < 10$$

$$f(\zeta) = 0.6262 + 0.172\log_{10}\zeta, \quad 0.001 < \zeta < 0.04$$
$$= 0.2784 - 0.2979\log_{10}\zeta - 0.06611(\log_{10}\zeta)^2$$
$$+ 0.10613(\log_{10}\zeta)^3 + 0.02531(\log_{10}\zeta)^4,$$
$$0.04 < \zeta < 10$$

$$= \tfrac{1}{2}\zeta, \quad \zeta > 10$$

where $v \equiv \log_{10}\epsilon$ and $\zeta = t^{1/2}$. The stopping power $S_{v>T}$ associated with nuclear-scattering processes in which more than some energy $T$ (keV) is transferred by a moving atom of energy $E$ (keV) was of interest here and requires a parameter $\lambda = (t^{1/2})_{min}$ (ergs),

$$\lambda = 17.466(M_2/M_1)^{1/2}Z^{-1/2}(Z_1Z_2)^{-1}(TE)^{1/2},$$

which was employed as follows:

$$S_{v>T} = [\epsilon^{-1}\int_\lambda^\epsilon f(\zeta)\,d\zeta](E/\epsilon)(\rho/R).$$

The range was calculated from
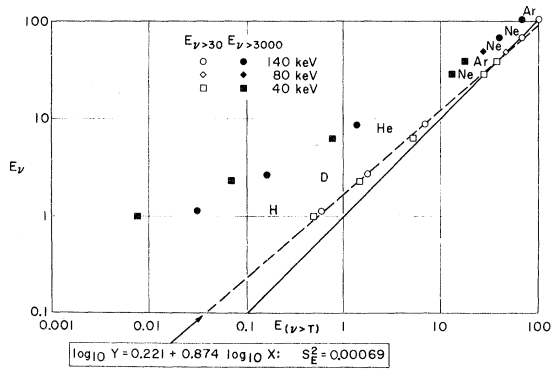
FIG. 1. Total energy dissipated in vitreous silica by atomic collisions plotted against the energy dissipated in atomic collisions in which more than a threshold energy is transferred. The full line is for threshold zero (slope unity). The dashed line is a logarithmic least-squares fit to data for a threshold of 30 eV.

$$R = \int_0^E S_T^{-1} dE ,$$

and the energy dissipated in nuclear-scattering processes was calculated from

$$E_{\nu > T} = \int_0^E S_{\nu > T} S_T^{-1} dE .$$

All the designated integrations were performed numerically by trapezoidal integration because analytical integration of the above approximations proved unsatisfactory. [13] The functions were tabulated and the tables were summed. The results of these calculations are presented in Table I.

It will be recognized that these calculations possess several deficiencies. They consider only pairwise interactions, they do not consider alternating interaction with silicon and oxygen, and they neglect secondary and back scattering. They also neglect the structure of the solid which possesses void space adjacent to oxygen, and hence would favor oxygen interactions over silicon interactions, particularly for moving particles of low energy. However, it is anticipated that these effects are minor compared to the uncertainty of the ionization stopping, particularly for the lightest ions. [14,15] The final digits in the tabulated results are of value only as guard digits in calculation; they are not significant. [16]

If a quantity which is proportional to the nuclear stopping were determined for various ions and energies and were plotted against the nuclear stopping on log-log paper, it is obvious that a line of slope unity would be obtained. To show the result of the quantity being proportional to the nuclear stopping in excess of a threshold, the logarithm of the stopping for thresholds of 30 and 3000 eV is plotted against the logarithm of the total nuclear stopping in Fig. 1. The results are curves. For the 30-eV threshold, the curve is nearly a straight

line with a 13% change in slope from unity. Thus, the slope of such a curve can be used to determine the threshold energy for the effect to within several eV. This procedure is of special merit here because compaction caused by ionization renders the usual procedure with fractional MeV electrons useless.

The data for vitreous silica presented in Table I are plotted against the nuclear stopping in Fig. 2. An unweighted logarithmic least-squares fit gives the result[17]

$$\log_{10} y = 1.401 + 1.027 \log_{10} E_{\nu(Tot)} .$$

If the data had been plotted against the nuclear stopping for a 30-eV threshold, the least-squares fit would be

$$\log_{10} y = 1.626 + 0.902 \log_{10} E_{\nu > 30} .$$

If the data which deviate greatly are discarded, the results obtained are

$$\log_{10} y = 1.451 + 0.981 \log_{10} E_{\nu(Tot)} ,$$

$$\log_{10} y = 1.635 + 0.881 \log_{10} E_{\nu > 30} .$$

If it is assumed that a layer the thickness of the Lindhard range $R_L$ calculated here suffers a dilatation $-0.027$ at saturation, for the heavier ions the maxima in the curves of dilatation vs charge correspond to ~60% of saturation. The rising portions of the curves have the form of an exponential
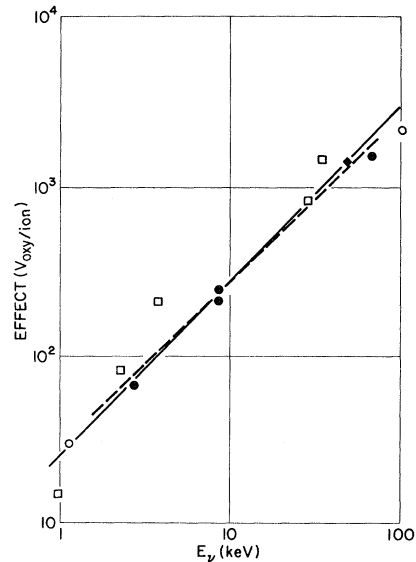


FIG. 2. Total negative dilatation associated with ions incident on vitreous silica plotted against the energy dissipated by the ions in atomic collisions. The filled points are the select points (see text); circles, 140 keV; diamonds, 80 keV; squares, 40 keV. The full line is a logarithmic least-squares fit to all the data; the dashed line is for the select data.

saturation at $\frac{3}{4}R_L$. However, since the radiation effects are not uniform with depth $x$, the true saturation curve is not exponential but an exponential integral; its character was investigated by examining the behavior of

$$\int_0^1 (1 - e^{-Q})\,dx$$

for various values of

$$\int_0^1 Q\,dx \ ,$$

where

$$Q = q\{1 - 0.2[1 + 71(x - 0.3)^2]^{1/2}\}$$

is an arbitrary function having the typical form of the depth dependence of the radiation effect; the independent variable for the calculation being $q$, the magnitude of $Q$ ($x$ is a dummy variable). This exponential integral is, at worst, but 5–10% lower than the exponential function; thus accounting for $\frac{1}{5}-\frac{1}{3}$ of the apparent low saturation value. The remainder must be accounted for largely by the stress relaxation[18]: the work of Hines and Arndt[19] (see below) indicates the layers affected by ion bombardment are close to the thickness of the Lindhard ranges calculated here. The analysis given here refers to the linear initial rate of the radiation effect. To obtain a correction for saturation, the percent of saturation for a particular ion was plotted against incident charge on log-log paper. A logarithmic least-squares fit was used to determine a "corrected" value for the quantity $\mu C/\text{deg}$ which was converted to units of $V_{\text{oxy}}/\text{ion}$ as described above. The behavior of these "corrected" values with ion energy was not satisfactory; it indicated an overcorrection. When these data were plotted against nuclear stopping, the results for $\log_{10} y$ were

all data:   $1.374 + 1.063\log_{10}E_{\nu(\text{Tot})}$,

$1.606 + 0.933\log_{10}E_{\nu>30}$ ;

select data:  $1.372 + 1.027\log_{10}E_{\nu(\text{Tot})}$,

$1.565 + 0.923\log_{10}E_{\nu>30}$ .

It is seen that the course of these curves is determined largely by the relative behavior of the various ions (which differs by orders of magnitude), and much less by the ion energy. Accordingly, errors in the data affect the results relatively little. The results indicate a threshold well below the 25–80 eV which has been determined for displacement thresholds in solids of this kind. Because of the uncertainties of the measurements (charge, see above; dilatation, see below), it cannot be stated with certainty that the threshold is negligible. However, the results do indicate that the compaction is caused by excitation of the solid rather than by being associated with displacements.

Since the stopping calculations would apply equally for other processes in silica, this procedure can be applied to the disordering of quartz for which Hines and Arndt[19] have published ion-bombardment data. They give an intensive quantity for the disordering, their $F_{50\%}$, the number of incident ions for which they observed a 50% completion of the refractive-index change calculated from their relative reflectivity measurements. If the range is divided by this, an extensive quantity proportional to the total effect is obtained. The thicknesses of the altered layers calculated by them from their reflectivity data correspond closely to the ranges calculated here for the Ne ions and ions of lower mass, and are much larger for Ar ions and ions of higher mass. Since their $F_{50\%}$ is employed here to calculate the relative total effect, their layer thicknesses were employed for consistency. The data are presented in Table II and are plotted in Fig. 3. The least-squares fits for the arbitrary placement of the origin $(x,y)$ at $(1, 10^{-18})$ are

$$\log_{10}y = -1.102 + 1.168\log_{10}E_{\nu(\text{Tot})} \ ,$$

$$\log_{10}y = -0.769 + 0.972\log_{10}E_{\nu>30} \ ,$$

indicating a threshold of 24.7 eV. This result supports the hypothesis that the radiation disordering of quartz requires atomic displacement, that it does not occur through excitation alone.

There are experimental uncertainties in both Hines and Arndt's data and in the present vitreous silicon data; e.g., the absolute rates of compaction for vitreous silica reported by them for $Ne^+$ (38 kev) do not agree with the ones reported here. Both their data and the present data show peculiar details of behavior for the heavier ions. Both the
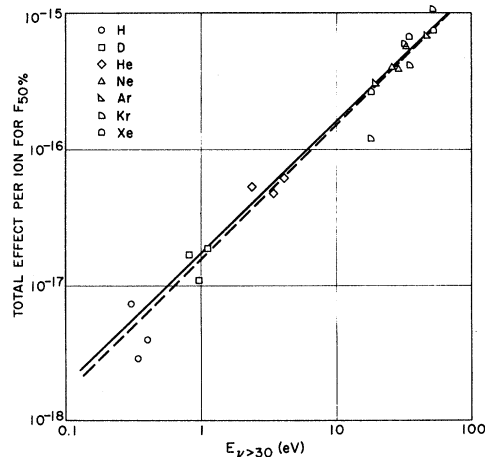


FIG. 3. Refractive-index data given by Hines and Arndt (Ref. 19) for ion bombardment of quartz treated in a manner similar to that employed in Fig. 2, but plotted against $E_{\nu>30}$. The dashed line is a best fit for slope unity; the full line is a logarithmic least-squares fit.

TABLE II. Reflectivity changes in quartz caused by ion bombardment (Ref. 15).

| Ion (energy) (keV) | Energy per nucleon (keV) | Layer thickness ($\mu$) | $F_{50\%}$ ($10^{14}$ ions/cm$^2$) | Relative total damage ($10^{-16}$) | Lindhard range ($\mu$) | Energy total nuclear (keV) | Dissipation nuclear >30 eV (keV) |
|---|---|---|---|---|---|---|---|
| $H_2^+$(14.6) | 7.3 | 0.171 | 234 | 0.0731 | 0.188 | 0.657 | 0.306 |
| (19.9) | 9.95 | 0.235 | 812 | 0.0289 | 0.226 | 0.720 | 0.345 |
| (32.6) | 16.3 | 0.338 | 846 | 0.0400 | 0.301 | 0.814 | 0.403 |
| $D_2^+$(12.8) | 6.4 | 0.219 | 130 | 0.168 | 0.201 | 1.35 | 0.815 |
| (18.8) | 9.4 | 0.290 | 266 | 0.109 | 0.263 | 1.56 | 0.960 |
| (29.6) | 14.8 | 0.400 | 220 | 0.182 | 0.355 | 1.80 | 1.129 |
| He$^+$ | 7.5 | 0.091 | 17.4 | 0.523 | 0.113 | 3.12 | 2.42 |
| | 15.1 | 0.191 | 39.9 | 0.478 | 0.197 | 4.45 | 3.55 |
| | 23.5 | 0.272 | 44.5 | 0.611 | 0.272 | 5.25 | 4.21 |
| Ne$^+$ | 38.3 | 0.074 | 1.85 | 4.0 | 0.073 | 27.8 | 26.5 |
| | 43.9 | 0.085 | 2.20 | 3.86 | 0.083 | 31.0 | 29.6 |
| | 51.8 | 0.095 | 1.68 | 5.65 | 0.098 | 35.2 | 33.7 |
| Ar$^+$ | 22.9 | 0.06 | 2.0 | 3.0 | 0.023 | 20.3 | 19.5 |
| | 38.4 | 0.07 | 1.20 | 5.8 | 0.037 | 33.1 | 32.1 |
| | 59.0 | 0.1 | 1.50 | 6.7 | 0.057 | 49.1 | 47.7 |
| Kr$^+$ | 20.3 | 0.050 | 4.2(?) | 1.19 | 0.013 | 19.0 | 18.1 |
| | 39.7 | 0.060 | 1.48 | 4.05 | 0.023 | 36.6 | 35.5 |
| | 59.0 | 0.067 | 0.62 | 10.81 | 0.032 | 53.7 | 52.5 |
| Xe$^+$ | 20.3 | 0.047 | 1.87 | 2.51 | 0.012 | 19.2 | 18.1 |
| | 39.4 | 0.053 | 0.81 | 6.54 | 0.019 | 36.9 | 35.6 |
| | 59.0 | 0.058 | 0.80 | 7.25 | 0.026 | 54.9 | 53.4 |

specimens studied here and those studied by them were lapped and polished. There is evidence that this surface finishing causes changes in refractive index and density.[20] Mechanical compaction can be affected by radiation. Particularly for the heavy ions whose ranges are very small and for protons whose stopping is largely through ionization, an alteration of the surface-polishing compaction on irradiation may affect the results seriously. This has yet to be investigated; clearly, additional data are needed. Also, more exact calculations of stopping should be made. However, the comparative behavior of these two cases supports the validity of the procedure presented here,

and it seems undesirable to delay reporting this investigation any longer, as the method and the results may be of interest to others. It is planned to apply the procedure to other cases as the opportunity arises.

A sequel[21] to this paper has appeared.

### ACKNOWLEDGMENTS

*Paper based on work performed under the auspices of the U. S. Atomic Energy Commission.

[1]W. Primak and R. Kampwirth, J. Appl. Phys. 39, 6010 (1968).

[2]W. Primak and R. Kampwirth, J. Appl. Phys. 39, 5651 (1968).

[3]W. Primak and R. Kampwirth, J. Appl. Phys. 40, 685 (1969).

[4]W. Primak and R. Kampwirth, J. Appl. Phys. 40, 2565 (1969).

[5]W. Primak, Surface Sci. 16, 398 (1969).

[6]W. Primak and R. Kampwirth, Appl. Opt. 10, 307 (1971).

[7]W. Primak, in Studies in Radiation Effects, edited by J. G. Dienes (Gordon and Breach, New York, to be published), Vol. IV.

[8]W. Primak and E. Edwards, Phys. Rev. 128, 2580

(1962).

[9]W. Primak, Nucl. Sci. Eng. 2, 117 (1957).

[10]J. Lindhard, M. Scharff, and H. E. Schiott, Kgl. Danske Videnskab. Selskab, Mat.-Fys. Medd. 33 (No. 14) (1963).

[11]J. Lindhard, V. Nielsen, and M. Scharff, Kgl. Danske Videnskab. Selskab, Mat.-Fys. Medd. 36 (No. 10) (1968).

[12]This section is not intended as an exposition of the range calculations given in Ref. 11; it is merely a compact statment of the arithmetic operations performed by the computer. The reader wishing to understand the formulas should read this section with Refs. 10 (particularly pp. 16–19) and 11 (particularly pp. 6–9) in hand. Their symbols have been retained here to facilitate such a reading despite a conflict, in some instances, with symbols which conform to the author's previous papers (Refs. 6 and 8) utilized in Sec. II. There $t$ is the thickness of the af-

fected layer, a kind of range; here it is a parameter proportional to energy transfer and particle energy. The function $f(\xi)$ is the reduced differential cross section calculated from the Thomas—Fermi potential (Ref. 10, pp. 17 and 18). The $\nu$ is a subscript to designate process involving atomic scattering and $\epsilon$ a subscript to designate ionization processes (Lindhard *et al.* use the words *nuclear* and *electronics*). Note the two usages for $T$ in the subscripts: This is the author's, not Lindhard's.

[13] Analytical integration of an approximation given in powers of the logarithm is usually unsatisfactory for numerical work, contrary to the usual experience that integrals of approximations are better than the approximations. The reader will recall that integration by parts is involved, and the result is a sequence of positive and negative terms of nearly equal magnitude, a disaster for numerical work. It proved more convenient with the facilities utilized by the author for the present work to use trapezoidal integration with a smaller interval than to use a more complex formula with a larger interval.

[14] B. Fastrup, A. Borup, and P. Hvelplund, Can. J. Phys. 46, 489 (1968).

[15] J. H. Ormrod, Can. J. Phys. 46, 497 (1968).

[16] The absolute accuracy of the range calculations in Refs. 10 and 11 is considered to be 20% at best, or one digit. For comparison purposes, as used here, it may be reasonable to utilize two digits. Obviously, no numerical work can be conducted with one digit because, even in hand computation, rounding errors are propagated at least one digit. In well-designed machine computation, where each individual operation cannot be supervised, it is found that rounding errors are propagated for two or three digits. It is therefore customary to retain at least two additional digits in such computations. Customarily, these are termed guard digits. It will be understood that in poorly designed computations, when small differences between large numbers arise, all significance may be lost even when retaining many more guard digits.

[17] Recall, only the slope of the log-log curve is significant in the following comparisons (v. s.).

[18] W. Primak, J. Appl. Phys. 35, 1342 (1964).

[19] R. L. Hines and R. Arndt, Phys. Rev. 119, 623 (1960).

[20] H. Yokota, H. Sakata, M. Nishibori, and K. Kinosita Surface Sci. 16, 265 (1969).

[21] W. Primak, J. Appl. Phys. 43, 2745 (1972).

# Dynamic Initial Slip in a Linear Chain

James Tasi

*Department of Mechanics, State University of New York, Stony Brook, New York* 11790

(Received 28 April 1972)

A linear Frenkel—Kontorova model is used to study, within the harmonic approximation, dynamic effects on the Peierls stress that occur when a dislocation is subjected to a shock wave. At large distances into the lattice, a small reduction in the Peierls stress can occur due to dynamic amplification of the peak stress associated with a dispersive shock wave. A larger reduction in the Peierls stress is shown to occur far behind the head of the incident wave and is due to the frequency-of-dislocation motion falling within the spectrum of frequencies that contribute to the stress wave. The reduction is the same as that which would occur if the dislocation were subject to a sudden step jump in stress. Finally, the effect of wave reflections along a slip plane is considered, and the unacceptable consequence of using a one-dimensional model in this last problem is demonstrated.

## I. INTRODUCTION

This paper is concerned with the dynamic effects on the Peierls stress that occur when a dislocation is subjected to a shock wave. The classical definition of a Peierls stress is assumed, i.e., the minimum shear stress required to move a straight-line dislocation, in an otherwise perfect crystal, past the potential barrier in a crystal and without any thermal assistance to initiate the motion. The modified linear Frenkel–Kontorova model[1] is used, with a dislocation subjected to nearest-neighbor interatomic forces along the direction of slip and also subjected to a piecewise linear substrate force. The one-dimensional chain model for slip used in the analysis is quite idealized physically. However, it yields analytical solutions in terms of the parameters that affect dislocation motion, and, as in static studies of Peierls stress,[2,3] can have some of the qualitative features of more realistic two-dimensional models.[4] Also, as in the static case, the discrete atomistic nature of the model yields effects that are not realized in a continuum model.

With the harmonic approximation for lattice motion, the rapid rise time of a shock wave cannot be maintained because of the dispersive response of an atomic structure. Hence, it has been assumed there are essentially no dynamic effects on Peierls stress after the wave has traveled a sufficient distance into the lattice. However, the very dispersion which lengthens the rise time of a shock